# 3D NONLINEAR MAGNETIZATION STUDIES OF THIN AMORPHOUS RIBBONS

**Richard L. Copeland and Markus B. Kopp**
Sensormatic Electronics Corporation
500 N.W. 12th Avenue
Deerfield Beach, Florida 33442

**Abstract**

Three-Dimensional analysis of a thin amorphous magnetic ribbon is studied using MSC/EMAS. A uniform static magnetic field is applied at various angles with respect to a nonlinear isotropic magnetic ribbon by using HSURF loads at certain boundary grid points. Different finite element meshes were examined in terms of generating a very uniform magnetic field to a region in the model center representing the thin amorphous ribbon. A simple uniform mesh produced a more uniform field than a mesh with much more refinement at the center. The importance of the proper boundary conditions along with the HSURF loads are discussed. The results clearly demonstrate the expected closure field around the ribbon and help in understanding the magnetization distributions in and around thin magnetic regions under an applied uniform field.

## Introduction

Thin amorphous ribbons have been used in many applications such as magnetometers[1], strain gauge sensors, position sensors, and security sensors[2]. Many studies treat the sensor material as a lumped equivalent circuit where the field in the material is assumed to be constant[3]. Others use 2D micromagnetic analysis to study magnetic domain distributions inside of the material assuming a constant applied field[4]. In this paper, we study the 3D magnetization using a uniform static magnetic field applied at various angles with respect to the easy axis of the sensor material. It is difficult to measure the magnetic field inside of the amorphous ribbon since a typical thickness is about 23 microns and the ribbon length and width are typically 38 mm and 13 mm respectively. It is especially of interest to know how the field in the ribbon changes when it is rotated with respect to the applied field. This is of practical interest in understanding the coupling of the excitation field from an antenna to a small sensor as the sensor is moved with respect to the applied field.

## 3D Model

In general, there are several ways of using MSC/EMAS to create a uniform applied magnetic field. A coil could be constructed around the object of interest and the geometry could be manipulated until the desired uniformity is obtained. The problem with this method is that a large air region may be required in order to avoid boundary condition generated error field gradients. Another method is using HSURF loads at several grid points on certain boundary regions with the proper boundary conditions and SPC constraints. This method can reduce the model size significantly while still generating a uniform applied field to the object. Figure 1 shows a drawing of this approach. The most appropriate boundary conditions for the vector potential A are shown on the boundary region faces. If the applied magnetic field is to be applied uniformly in the x direction to the object, then since $B = \nabla \times A$, the normal component of A, $A_n$, should be set to zero at these boundary surface regions. HSURF loads are placed at grid points on the ends of the model as shown in Figure 1 with the excitation in the x direction. Since these HSURF loads specify the magnetic field at these grid points, the SPC constraints cannot be placed on any of these grids. For best results, the boundary surfaces where the HSURF loads are placed should be left unconstrained. The top and bottom boundary surfaces should have the tangential component of A, $A_t$, set to zero.

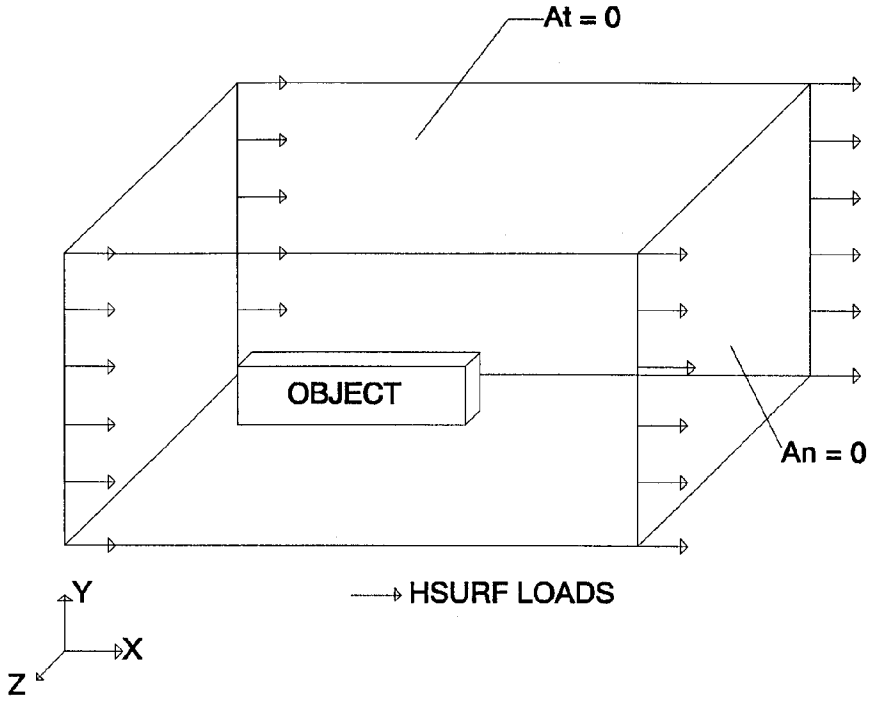


Figure 1. HSURF loads on boundary regions and boundary conditions for uniform magnetization applied to object in x direction.

**Uniform Magnetization Case**

Figure 2 shows the first 3D finite element mesh used for the uniform magnetization case. First order finite elements were used in all cases. The thin rectangular region in the middle of the mesh is the ribbon. Just enough air elements were placed around this material to allow for field closure around this material under the applied HSURF field.

Figure 3 shows the nonlinear BH curve for the amorphous magnetic ribbon. This material is Allied Metglas alloy 2826MB which has excellent magnetoelastic properties.

Figure 4 shows the arrow plot for the magnetic field in air. The plane of 3D hexehedra elements representing the ribbon plane are shown here. Here, the magnetic material properties were set to air in order to study the ability of this model to produce a uniform applied field. A very uniform field is observed.

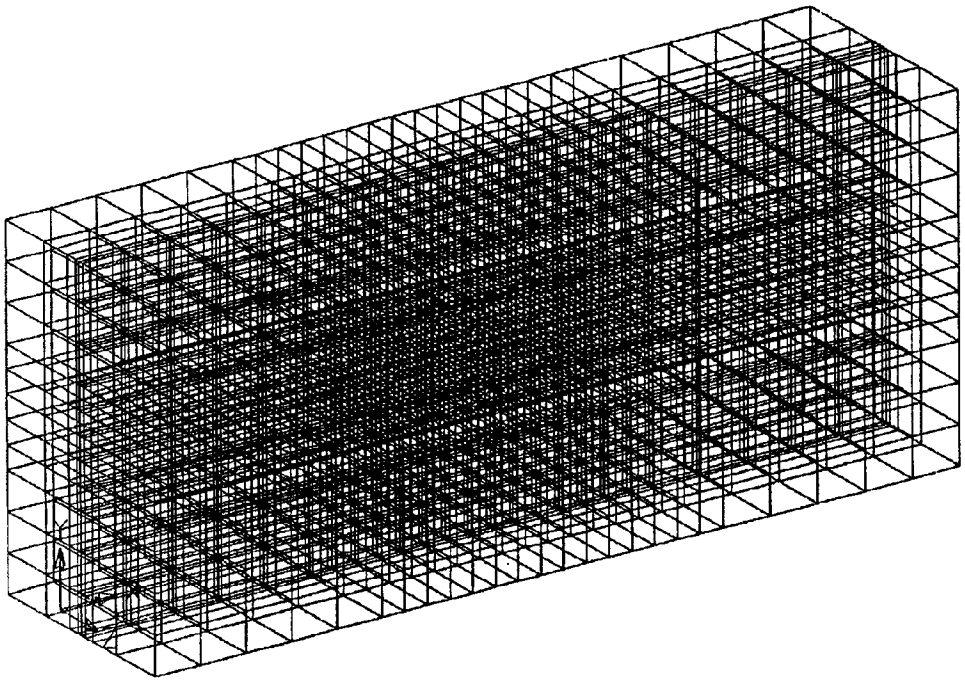

Figure 2. First 3D finite element mesh used for the uniform magnetization case.

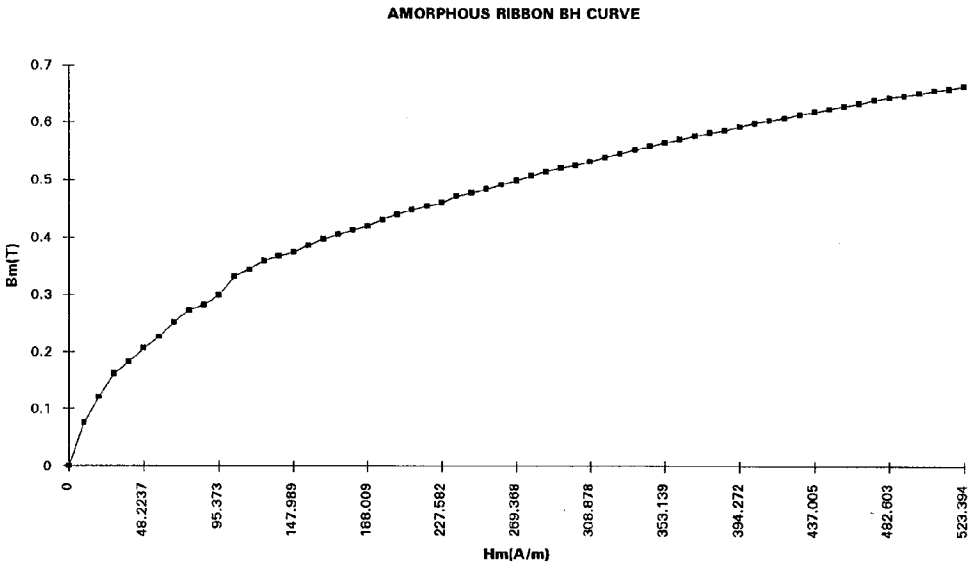


Figure 3. Nonlinear BH curve for amorphous ribbon material.

Figure 5 shows the arrow plot for the H field for the same plane as in Figure 4 with the nonlinear ribbon material present. Note the field closure around

the ribbon due to the finite ribbon length. The applied field causes a longitudinal dipole field which perturbs the local applied field. The important point here is that the H field is fairly uniform through the magnetic material.

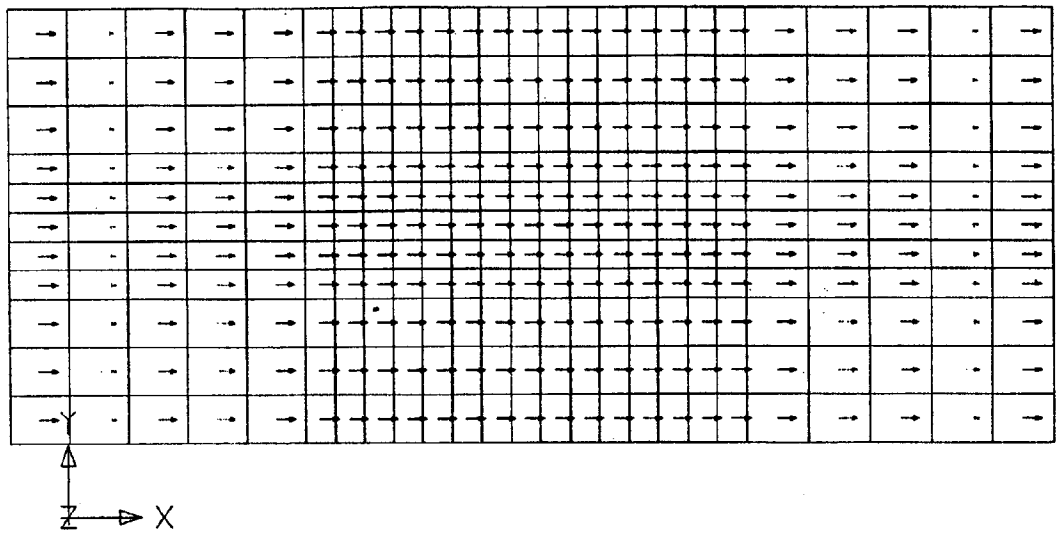


Figure 4. Arrow plot for the magnetic field in air.

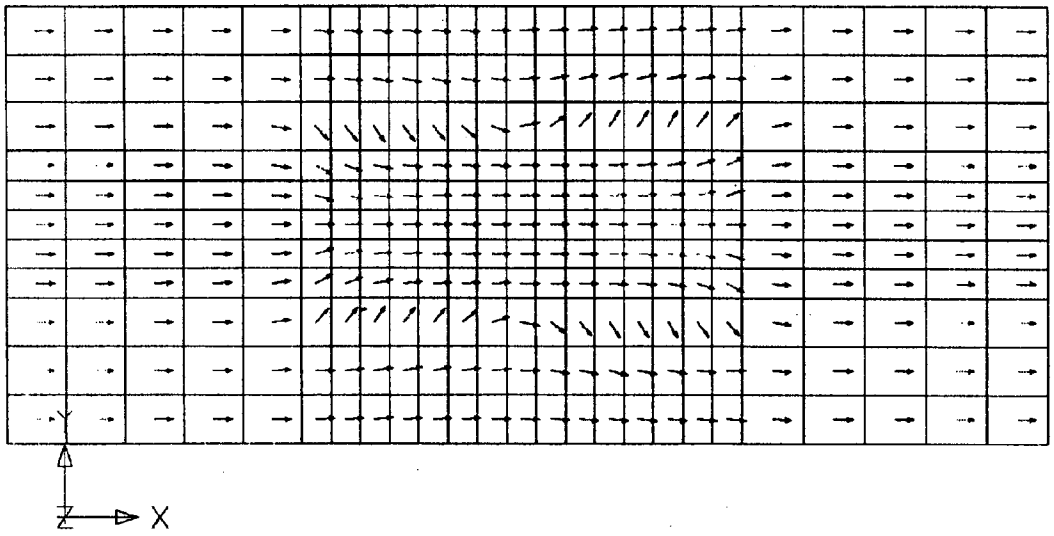


Figure 5. Arrow plot for the H field for the same plane as in Figure 3 with the nonlinear ribbon material present.

Next, we studied a more refined mesh to see if improvement could be obtained. Figure 6 shows the arrow plot of the magnetic field in air for this model. Again, only the 3D hexahedra elements representing the ribbon material plane are shown. Here, even though the field is fairly uniform,

there is some definite waviness in the field surrounding the ribbon elements and throughout the ribbon. We feel that this is caused by the particular mesh which starts out relatively large at the boundaries and is refined as the ribbon elements are reached.

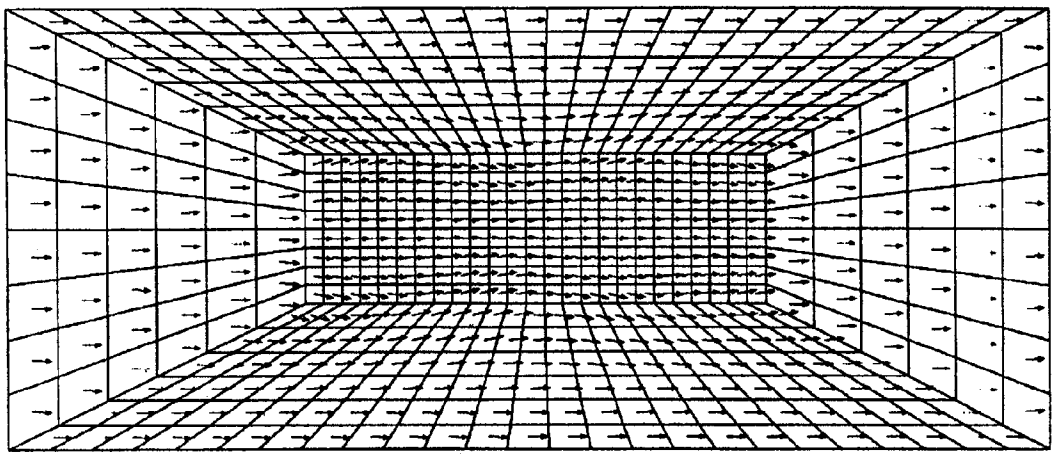

Figure 6. Arrow plot of the magnetic field in air for more refined mesh model.

Figure 7 shows the arrow plot for the H field with the ribbon material present. The presence of the magnetic properties causes the H field to become more uniform. So, the results here appear to be very realistic. Again, the closure fields can readily be observed. Figure 8 shows a blowup of the fields in the ribbon material only.

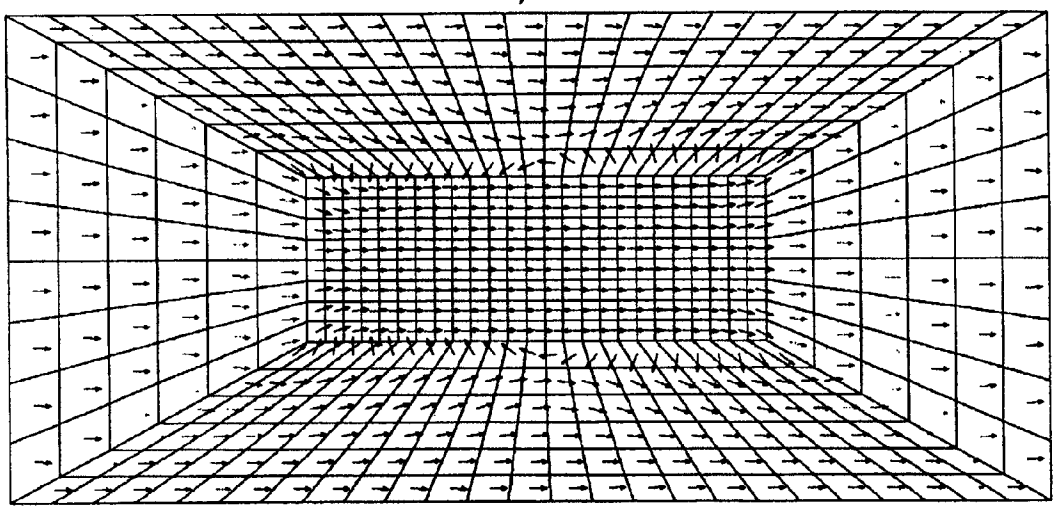

Figure 7. Arrow plot for the H field with the ribbon material present.

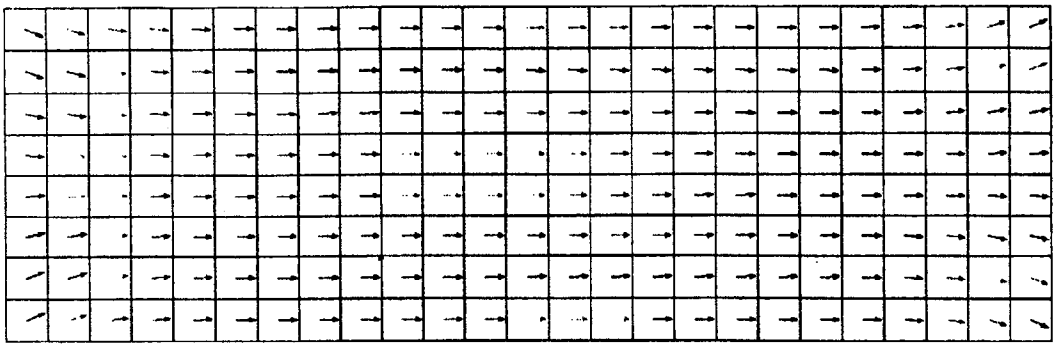

Figure 8. Blowup of the fields in the ribbon material only.

## Magnetization at Various Angles

Next, we wanted to study magnetization at some small angle. One obvious way of achieving this is to create a new mesh with the same number of elements and grid points, but to rotate the ribbon about the model center 10 degrees. We started off using the more refined mesh approach as before. Figure 9 shows the arrow plot of the magnetic field for the air case. Due to the extreme distortion in this mesh the uniformity of the fields is very poor. At the outside boundary regions the field is well behaved, whereas the field in the model center where the ribbon is located is very distorted.

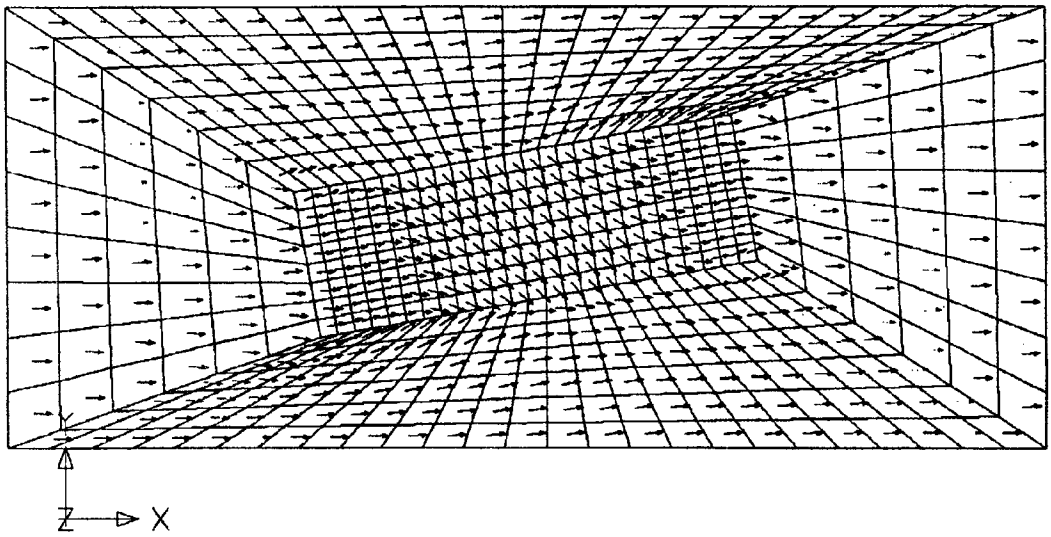


Figure 9. Arrow plot of the magnetic field for the air case with rotated refined mesh.

A more uniform mesh was tried for this 10 degree angle case. Figure 10 shows the arrow plot for the magnetic field for this newer mesh for the 3D hexahedra elements in the ribbon plane. This is the solution for the air only

case. Here we can see a very uniform field distribution throughout the model.

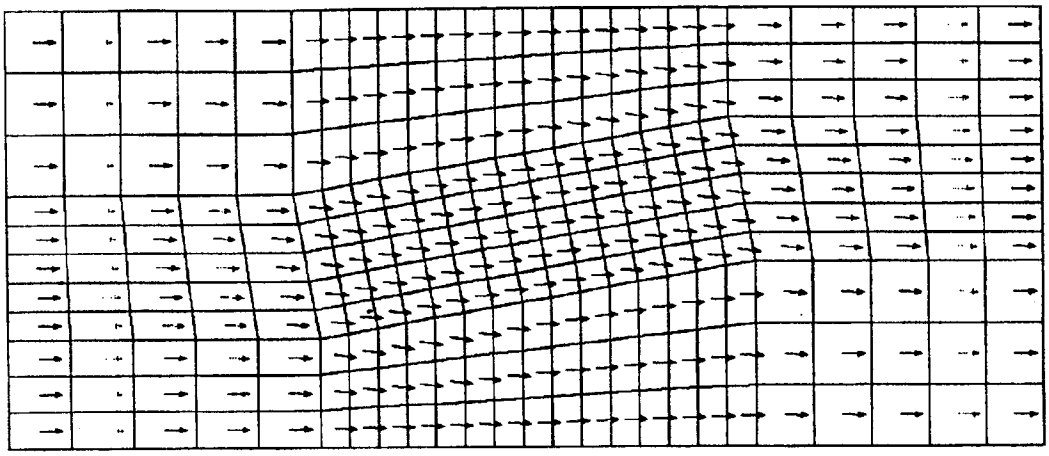

Figure 10. Arrow plot for the magnetic field in air for newer mesh.

Figure 11 shows the arrow plot for the H field for the 3D elements in the ribbon plane with the magnetic properties applied. Due to the angle of the applied field to the material, the field lines follow the ribbon axis for the central part of the ribbon but there is much more curvature in the magnetic field inside of the material in this case.

Figure 12 shows a blowup of the field for the ribbon elements only.

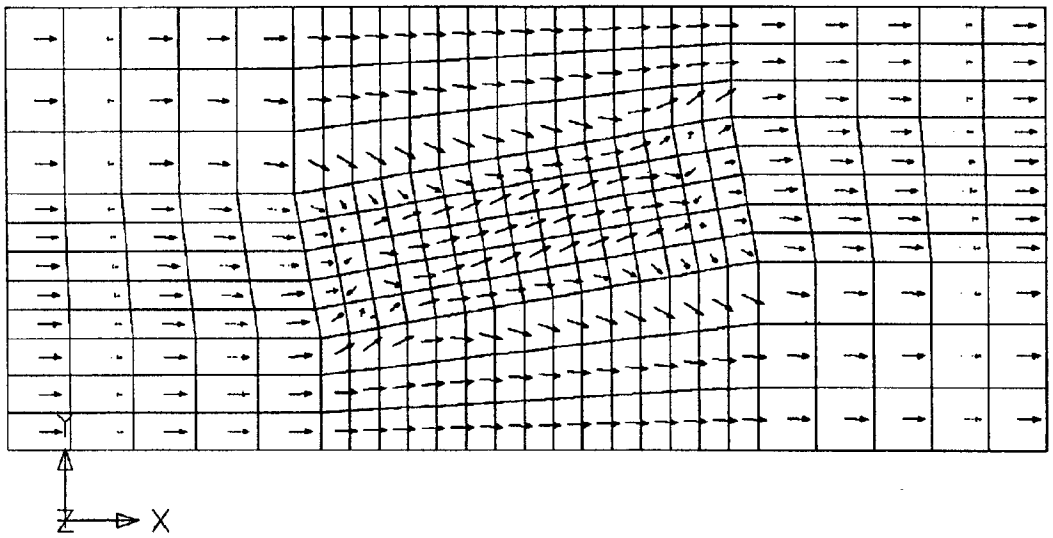


Figure 11. Arrow plot for the H field for the 3D elements in the ribbon plane with the magnetic ribbon present.

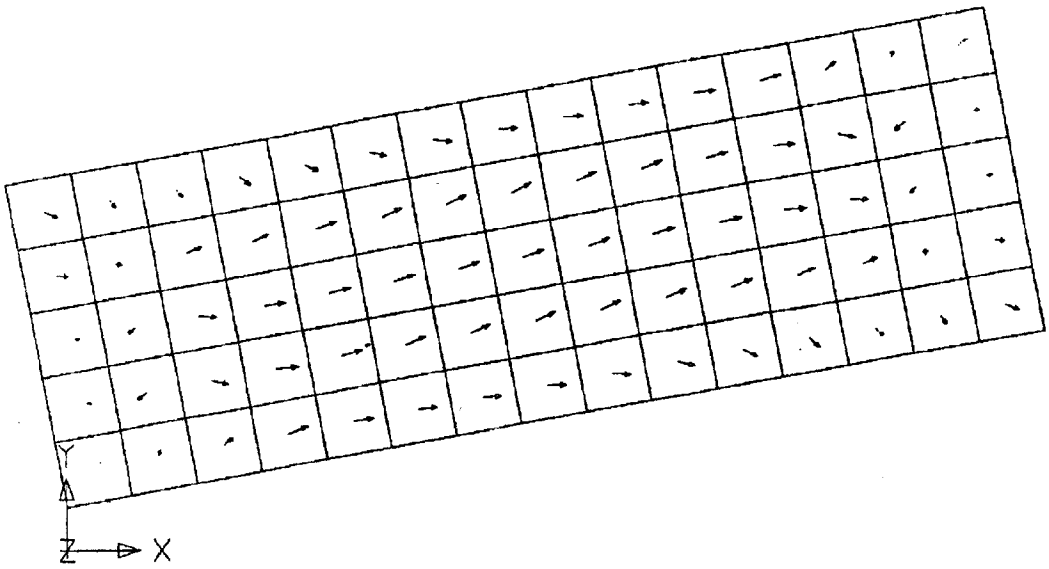

Figure 12. Blowup of the field for the ribbon elements only.

## Alternate Methods

Instead of changing the finite element mesh to rotate the ribbon with respect to the applied field, another possible way to do this without as much work was suggested by Chuck Figer of MSC. If the grid points where the HSURF elements were applied were assigned a new coordinate system which is rotated and the constraints also had this new coordinate system, then it should be possible to apply an angular field to the interior mesh region. An example of this technique[5] was brought to our attention by Pat Lamers of MSC for a 3D linear magnetostatic example of a steel cylinder with applied field at various angles with good results.

We tried this technique for the more refined mesh with no material rotation without success. This technique in general should work and could simplify the problem but may be sensitive to mesh geometries.

## Conclusions

We have demonstrated some simple techniques that can be used to generate a uniform applied field to a thin magnetic ribbon using MSC/EMAS. We used the example of a magnetic amorphous ribbon since we are familiar with the expected results and this paper is purely theoretical. We found that for the case where the ribbon axis and the applied field are aligned, the results are similar for both the simple uniform mesh and a more refined mesh. However, when the ribbon is rotated with respect to the applied field, the less refined more uniform mesh produced more realistic results.

The effect of field closure caused by the dipole field along the magnetic ribbon material is clearly demonstrated. This shows how the local applied field is perturbed by the magnetic ribbon material.

## References

[1]M. D. Mermelstein, "A magnetoelastic metallic glass low-frequency magnetometer" , IEEE Transactions on Magnetics, vol. 28, no. 1, January, 1992.

[2]R. C. O'Handley, "Magnetic materials for sensors", Proceedings of the ASTM Conference, Chicago, November 4, 1992.

[3]S. Butterworth and F. D. Smith, "The equivalent circuit of the magnetostriction oscillator", Physics Society, XLIII, 2, pp166-185, 1931.

[4]Neil Smith, "Micromagnetic analysis of a coupled thin-film self-biased magnetoresistive sensor", IEEE Transactions on Magnetics, vol. 23, no. 1,January, 1987.

[5]H. C. Janzen and F. Hirtenfelder, "MSC/EMAS EMI & Crosstalk Example 3: Shielding Problem", MacNeil-Schwendler Corp. Electromagnetic Applications Dept. Report, September, 1992.